JPE 18-4-12

https://doi.org/10.6113/JPE.2018.18.4.1075
ISSN(Print): 1598-2092 / ISSN(Online): 2093-4718

Finite-Time Nonlinear Disturbance Observer Based Discretized Integral Sliding Mode Control for PMSM Drives

Changming Zheng† and Jiasheng Zhang*

†,*College of Information and Control Engineering, China University of Petroleum (East China), Qingdao, China

Abstract

To deal with the operation performance degradation of permanent magnet synchronous machine (PMSM) drives with uncertainties and unmodeled dynamics, this paper presents a finite-time nonlinear disturbance observer (FTNDO) based discretized integral sliding mode (DISM) composite control scheme. Based on the reaching-law approach, a DISM speed controller featuring a superior dynamic quality and global robustness against disturbances is constructed. This controller can avoid the reaching phase and overlarge control action. In addition, a sliding mode differentiator based FTNDO is devised and extended to the discrete-time domain for disturbance estimation. The attractive features of the FTNDO are that it can provide a finite-time converging estimation and alleviate the chattering effect in conventional sliding mode observers, while retaining robustness to parameter variations. By feeding the estimate forward to the pre-stage DISM controller, both disturbances and chattering can be significantly suppressed. Moreover, considering the estimation error of a FTNDO caused by discrete sampling, a stability analysis of the composite controller is discussed. Experimental results validate the superiority of the presented scheme.

Key words: Discrete sliding mode control, Finite-time observer, Permanent-magnet synchronous machine drives

I. INTRODUCTION

High-performance permanent magnet synchronous machines (PMSMs) have been extensively utilized in industrial sectors due to its compact structure and high power-to-weight ratio. As is well known, conventional PI control is still prevalent in PMSM due to its simplicity. Nevertheless, industrial PMSM drives are complex systems with various uncertainties and disturbances, which can result in the deterioration or even failure of PI algorithms [1]. Hence, enhancing dynamic responses while not weakening robustness is still a serious challenge.

Various control algorithms have been put forward to solve the above problems, including predictive strategies [2], adaptive strategies [3], and sliding mode control (SMC) strategies [1], [4], etc. Among them, SMC is known as an approach featuring simple implementation, superior dynamic performance and invariance property to disturbances or uncertainties. Note that the SMC algorithms were initially devised in the continuous-time domain, i.e., the continuous-time SMC (CSMC). However, nowadays most control algorithms are digitally implemented on computers. Considering that the sampling time cannot be infinitely small, the control input of the CSMC is frozen during a sampling period and the invariability of the CSMC is degraded or even invalid [5]. Hence, straightly employing the CSMC to the discrete-time domain without any modification can result in unexpected problems. Thus, research on discretized SMC (DSMC) is inevitable. Many DSMC algorithms have been presented and successfully applied in PMSMs [6]-[8]. Nevertheless, in the conventional DSMC, the order of the dynamics model is decreased and the differential terms are introduced to magnify the noises. To overcome these defects, discretized integral SMC (DISMC) algorithms have been presented and employed in motion tracking systems [9]-[11]. However, they have rarely been used for PMSM drives. In addition, the DISMC algorithms designed above are often based on equivalent control with a switching term, which

Manuscript received Aug. 24, 2017; accepted Mar. 3, 2018
Recommended for publication by Associate Editor Dong-Hee Lee.
†Corresponding Author: jsxzzcm@126.com
Tel: +86-15698112301, China University of Petroleum
*College of Information and Control Engineering, China University of Petroleum (East China), China

cannot achieve an excellent dynamic quality and may cause an overlarge control effort when disturbances occur [12]. Moreover, the sliding surface of the DSMC can only move into a quasi-sliding mode (QSM) domain instead of moving onto the ideal sliding surface [6]. In addition, the switching gain should be chosen sufficiently large to guarantee the reachability of the QSM, which induces chattering. Since chattering can attenuate control accuracy, many chattering suppression methods have been presented, where the reaching-law approaches and high-order SMC have proved to be the most efficient [6], [13]. The reaching-law approaches can directly regulate the convergence rate during the reaching phase to suppress chattering. The high-order SMC algorithms can essentially alleviate chattering while not degenerating robustness. The most common one is a second-order sliding mode algorithm (2-SMA). The 2-SMA has been successfully utilized in identification, observation and differentiation [14]-[17]. In addition, to further enhance the chattering alleviation and anti-disturbance performance of SMC-based control systems, disturbance or uncertainty estimation and attenuation (DUEA) methods are increasingly used [18]. These techniques share a similar principle, which is constructing an observer for disturbance estimation and generating the corresponding compensation by using the estimate. The commonly-used DUEA methods for PMSM drives include the sliding mode disturbance observer (SMDO), extended state observer (ESO) and disturbance observer (DO), [1]-[3], [19]. However, the estimation accuracy of the DO and ESO is more or less influenced by parameter variations, and they have a common disadvantage in terms of asymptotic convergence. Note that convergence in finite time is an attractive property, which means a faster convergence rate and a higher accuracy. An extended SMDO with a finite-time convergence rate for PMSM drives was presented in [1]. However, chattering is inevitable and a low-pass filter (LPF) is introduced for chattering attenuation, which causes a phase delay and deterioration of the observation performance.

This paper presents a DISMC scheme with a finite-time nonlinear DO for PMSM drives. An integral-type nonlinear sliding surface is introduced and a discretized integral sliding-mode (DISM) speed controller is constructed using the reaching-law approach. The initial reaching phase of the DISM can be eliminated and global robustness can be obtained when the initial value of the sliding function is properly configured. Moreover, motivated by the 2-SMA based sliding mode differentiator technique, a discretized finite-time nonlinear DO (FTNDO) is presented to provide finite-time converging estimation of the lumped disturbance for PMSM drives. Another unique feature of the FTNDO is that it can alleviate chattering behavior in the conventional SMDO without losing robustness to parameter variations. In addition, in view of the discretized estimation error, the stability of the composite controller is analyzed theoretically. Finally, the superior dynamic responses and anti-disturbance capabilities of the presented algorithm are verified by experiments.

The remainder of this paper is arranged as follows. Section II constructs a discrete dynamics model of the PMSM with the lumped disturbance. The design procedures of the FTNDO-DISMC scheme are elaborated in Section III, where a stability analysis of the composite controller is also given. Experimental results and comparisons are investigated in Section IV, and some conclusions are given in Section V.

II. Dynamics Model of a PMSM with Lumped Disturbance

In the rotor d–q synchronous rotating coordinate system, the nominal dynamics model of a non-salient PMSM with no saturation of the magnetic circuit can be described as:

$$J\dot{\omega}_r(t) + B_f\omega_r(t) = K_t i_q(t) - T_L(t) \tag{1}$$

where $K_t = 1.5p\psi_f$ donates the torque constant. p and ψ_f donate the pole pairs and flux linkage, respectively. $i_q(t)$ is the q-axis current and $K_t i_q(t)$ represents the electromagnetic torque T_e. The parameters J, B_f and $T_L(t)$ donate the rotational inertia, friction coefficient and load torque, respectively. ω_r (t) donates the mechanical angular velocity.

Taking the parameter uncertainties and unmodeled dynamics as the equivalent lumped disturbance of a PMSM, the continuous-time scalar dynamics model of the PMSM in equation (1) can be obtained by:

$$\dot{X}(t) = A_c X(t) + B_c u(t) + d(t) \tag{2}$$

$$d(t) = \Delta A_c X(t) + \Delta B_c u(t) - T_L(t)/J \tag{3}$$

where $X(t) = \omega_r$ and $u(t) = i_q$. $A_c = -B_f/J$ and $B_c = K_t/J$ denote the scalar nominal parameters. ΔA_c and ΔB_c donate the parameter uncertainties. $d(t)$ donates the lumped disturbance, including uncertainties, unmodeled disturbances and load torque disturbances.

Considering that the sampling period T is very small, the Euler difference method can be employed for approximate discretization.

$$\dot{X}(t) \approx \frac{X_{k+1} - X_k}{T} \tag{4}$$

where $X_k = X(kT)$, and k donates the kth time step.

Moreover, applying equation (4) into equation (2), the discretized form of the PMSM dynamics model with lumped disturbance can be obtained by:

$$X_{k+1} = AX_k + Bu_k + f_k \tag{5}$$

where $u_k = u(kT)$, with the scalar parameters:

$$A = TA_c + 1,\ B = TB_c \tag{6}$$

$$f_k = Td_k,\ d_k = d(kT) \tag{7}$$

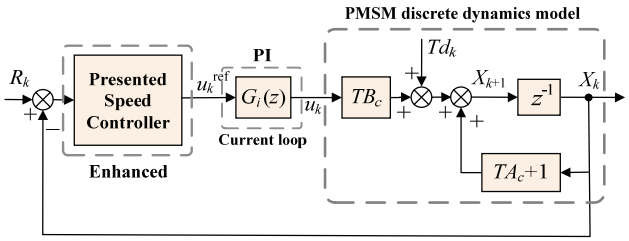

Fig. 1. Overall structure of a discrete PMSM regulation system.

For conventional field-oriented control (FOC) based PMSM drive systems, this paper aims to devise an enhanced speed controller featuring fast dynamic responses, high precision and anti-disturbance performance. The current loops still use PI control. An overall block diagram of a PMSM dynamic system using the presented speed controller in the discrete-time domain is described in Fig. 1. Additionally, if the friction coefficient B_f is considered to be 0, or the first item on the right side of equation (2) is regarded as one part of the lumped disturbance $d(t)$, then, $A_c = 0$. Hence, the aforementioned two cases are essentially equivalent, and the speed controller design can be simplified.

III. Presented DISMC with Finite-Time Nonlinear DO

In this section, the specific design procedures of the presented FTNDO-DISMC scheme based on the PMSM discrete model in Section II are elaborated. First, a reaching-law based DISM speed controller is presented. Then, a SMD-based FTNDO is constructed to realize the finite-time converging estimation of the lumped disturbances. Finally, the presented composite control law is obtained and the stability is analyzed.

A. DISM Speed Controller Design

First, the tracking error of the speed can be defined as:

$$E_k = R_k - X_k \tag{8}$$

where R_k represents the speed reference ω_r^{ref}.

Then, a discretized nonlinear integral-type sliding surface is constructed as [9]:

$$S_k = ME_k + \kappa_k \tag{9}$$

$$\kappa_k = \kappa_{k-1} + GE_{k-1} \tag{10}$$

where S_k is the discretized sliding surface or sliding function. κ_k donates the error integral term aiming to eliminate the tracking error E_k. M and the integral gain G are the positive parameters to be designed.

To facilitate the DISM controller design, consider the one-step forward expression of equation (9) as:

$$\begin{aligned} S_{k+1} &= ME_{k+1} + \kappa_{k+1} \\ &= M(R_{k+1} - X_{k+1}) + \kappa_k + GE_k \end{aligned} \tag{11}$$

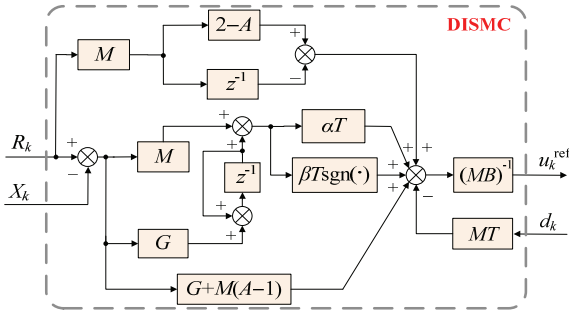

Fig. 2. Block diagram of the presented DISM controller.

Generating the expressions of X_{k+1} and κ_k from equations (5) and (9), and substituting them into (11) yields:

$$S_{k+1} = M(R_{k+1} - AX_k - Bu_k - f_k) + S_k + (G - M)E_k \tag{12}$$

Note that the tracking responses and chattering suppression using the reaching-law approach are better than equivalent control. In addition, the over-large control effort can be avoided. Considering the following discrete-time exponential reaching law presented by Gao *et al.* [6]:

$$S_{k+1} = (1 - \alpha T)S_k - \beta T\,\text{sgn}(S_k) \tag{13}$$

where $\alpha > 0$, $\beta > 0$ and $0 < 1 - \alpha T < 1$.

Substituting equation (13) into equation (12), by eliminating the left term S_{k+1}, the initial form of the desired control input u_k^{ref} can be obtained by:

$$\begin{aligned} u_k^{ref} = (MB)^{-1}[&MR_{k+1} - MAX_k - Mf_k + (G - M)E_k \\ &+ \alpha TS_k + \beta T\,\text{sgn}(S_k)] \end{aligned} \tag{14}$$

Normally, the frequency of R_k is much smaller than the sampling frequency, and its variation can be considered linear during a sampling period. Hence, the future R_{k+1} can be approximately predicted according to its previous values.

$$R_{k+1} \approx 2R_k - R_{k-1} \tag{15}$$

Substituting equation (15) into equation (14), a necessary simplification yields the command current of the DISM controller.

$$\begin{aligned} u_k^{ref} = (MB)^{-1}\{&M(2 - A)R_k - MR_{k-1} - MTd_k \\ &+ \alpha TS_k + \beta T\,\text{sgn}(S_k) + [G + M(A - 1)]E_k\} \end{aligned} \tag{16}$$

A block diagram of the presented DISM controller is shown in Fig. 2. Note that different initial values of κ_k in equation (9) can affect the system performance. On the one hand, if the initial speed tracking error E_0 is available, by setting the initial integral value to $\kappa_0 = -ME_0$, then $S_0 = 0$. This means the system trajectory stays in the QSM domain when $k = 0$. Hence, the initial reaching process towards the QSM is eliminated and global robustness can be obtained, which can improve the dynamic responses. On the other hand, if E_0 is unknown and κ_0 is set to a certain value that makes $S_0 \neq 0$, the initial system trajectory does not stay in the QSM and the reaching phase is introduced. Nevertheless, the presented

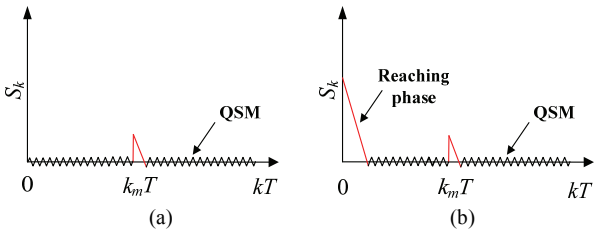

Fig. 3. Comparisons of S_k with different initial values: (a) $S_0 = 0$; (b) $S_0 \neq 0$.

control law of equation (16) is still applicable. Intuitive comparisons of S_k with different initial values are shown in Fig. 3, where a disturbance occurs at k_mT. The only difference is whether the initial reaching phase exists. Additionally, when a disturbance occurs during the sliding motion, the system trajectory is still driven towards the QSM domain with excellent dynamic quality by using the reaching-law approach.

B. Finite-Time Nonlinear Disturbance Observer Design

It can be observed from the control law of equation (16) that the lumped disturbance d_k is unknown and difficult to measure in practice, i.e., the current form of (16) cannot be directly implemented. To overcome this dilemma, a sliding-mode differentiator (SMD) based finite-time nonlinear DO is constructed to accurately estimate d_k online without adding extra hardware.

1) SMD-Based Observer

The 2-SMA based SMD, which can provide a finite-time convergence rate, preserve the strong insensitivity to parameter perturbations and remove the chattering effect of the conventional SMC, has been presented by Levant in [13], [14], [16] and [17]. Herein, the SMD-based finite-time DO is introduced in its simplest form with uncertainties and disturbances as:

$$\begin{cases} \dot{\hat{x}}(t) = u(t) + v(t) \\ v(t) = -\lambda_0 \left|\hat{x}(t) - x(t)\right|^{1/2} \operatorname{sgn}[\hat{x}(t) - x(t)] + \hat{z}(t) \\ \dot{\hat{z}}(t) = -\lambda_1 \operatorname{sgn}[\hat{z}(t) - v(t)] \end{cases} \tag{17}$$

where $x(t)$ and $z(t)$ donate the system state variable and disturbance, respectively. $\hat{x}(t)$ and $\hat{z}(t)$ donate the corresponding estimates. λ_0 and λ_1 are positive observer parameters. Then $\hat{x}(t) = x(t)$ and $\hat{z}(t) = z(t)$ can be obtained in finite time.

Considering digital implementation, similar to the treatment in equation (4), the discretized form of the finite-time DO is expressed as:

$$\begin{cases} \hat{x}_{k+1} = \hat{x}_k + T(u_k + v_k) \\ v_k = -\lambda_0 \left|\hat{x}_k - x_k\right|^{1/2} \operatorname{sgn}(\hat{x}_k - x_k) + \hat{z}_k \\ \hat{z}_{k+1} = \hat{z}_k - T\lambda_1 \operatorname{sgn}(\hat{z}_k - v_k) \end{cases} \tag{18}$$

A detailed stability analysis of the SMD-based observer in the continuous-time system has been discussed in [13], [16], where the stability condition assuring finite-time convergence is presented as:

$$\begin{cases} \lambda_0{}^2 \geq 4L \dfrac{\lambda_1 + L}{\lambda_1 - L} \\ \lambda_1 > L \end{cases} \tag{19}$$

where L donates the Lipshitz constant.

However, the stability condition of equation (19) in the continuous-time domain is rough. It is sufficient but not a necessary condition for the discrete-time domain. Stability discussions of the discretized SMD-based observer have been discussed in [20]-[21]. Moreover, the necessary and sufficient stability condition for the discrete sliding mode is given by [22]:

$$\left|\tilde{x}_{k+1}\right| \leq \left|\tilde{x}_k\right| \tag{20}$$

which can be decomposed into the following two inequalities:

$$\begin{cases} (\tilde{x}_{k+1} - \tilde{x}_k)\operatorname{sgn}(\tilde{x}_k) < 0 \\ (\tilde{x}_{k+1} + \tilde{x}_k)\operatorname{sgn}(\tilde{x}_k) \geq 0 \end{cases} \tag{21}$$

where $\tilde{x}_k = \hat{x}_k - x_k$ donates the estimation error.

Therefore, the stability of the discretized SMD-based observer can be guaranteed if the observer parameters λ_0 and λ_1 satisfy the inequalities of equation (21) and the conditions presented in [20], [21]. Then, the system trajectories of the finite-time DO can achieve the QSM within finite time steps and can stay in it indefinitely.

The estimation error bounds of the finite-time DO caused by discretization, without input noises, are given in [13], [16], [17] and [20]:

$$\begin{cases} \left|\hat{x}_k - x_k\right| \leq \gamma_1 T^2 \\ \left|\hat{z}_k - z_k\right| \leq \gamma_2 T \end{cases} \tag{22}$$

where γ_1 and γ_2 are positive constants depending on the observer gains λ_0 and λ_1.

In addition, considering the sampling error of the speed and currents, the estimation error of the finite-time DO is bounded by [13], [17]:

$$\begin{cases} \left|\hat{x}_k - x_k\right| \leq \delta_1 \psi \\ \left|\hat{z}_k - z_k\right| \leq \delta_2 \psi^{1/2} \end{cases} \tag{23}$$

where $\psi > 0$ donates the upper bound of the sampling error. δ_1 and δ_2 are positive constants depending on the observer gains λ_0 and λ_1.

2) Finite-Time Nonlinear DO for PMSM Drives

Based on equivalent substitution, regarding the X_k and d_k in equation (5) as the corresponding x_k and z_k in equation (18), by employing the discretized SMD-based DO in equation (18) to the PMSM discrete dynamics model of equation (5), the presented FTNDO for PMSM disturbance estimation can be constructed as:

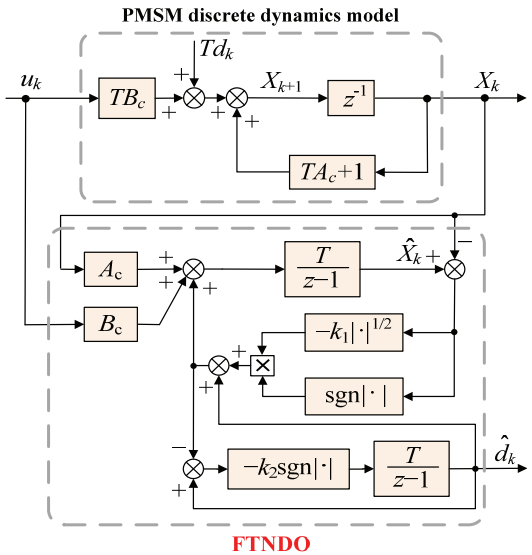

Fig. 4. Block diagram of the discretized FTNDO.

$$\begin{cases} \hat{X}_{k+1} = \hat{X}_k + T[-k_1\left|\hat{X}_k - X_k\right|^{1/2}\operatorname{sgn}(\hat{X}_k - X_k) \\ \qquad + A_c X_k + B_c u_k + \hat{d}_k] \\ \hat{d}_{k+1} = \hat{d}_k - Tk_2\operatorname{sgn}[k_1\left|\hat{X}_k - X_k\right|^{1/2}\operatorname{sgn}(\hat{X}_k - X_k)] \end{cases} \tag{24}$$

where k_1 and k_2 represent positive observer parameters. $\hat{X}_k$ and $\hat{d}_k$ donate the estimated ω_r and the lumped disturbance.

From equation (24), it can be concluded that the chattering effect can be alleviated through equivalent discrete integration. A block diagram of the implementation of the FTNDO in the discrete-time domain is depicted in Fig. 4.

C. DISMC with FTNDO

Since the unknown lumped disturbance d_k in equation (16) has been estimated by the FTNDO, by substituting the estimated $\hat{d}_k$ in equation (24) into equation (16), the entire control law of the FTNDO-DISMC can be obtained by:

$$\begin{aligned} u_k^{\text{ref}} = (MB)^{-1}\{&M(2-A)R_k - MR_{k-1} - MT\hat{d}_k \\ &+\alpha TS_k + \beta T\operatorname{sgn}(S_k) + [G + M(A-1)]E_k\} \end{aligned} \tag{25}$$

Moreover, it should be noted that the sign function in equation (25) induces unexpected chattering, which can affect the system performance. Although the adopted reaching-law approach can reduce the chattering to some extent, a smooth nonlinear function can also be used to continue the sign function in equation (25) for further chattering attenuation, that is:

$$\phi_k = \frac{S_k}{|S_k| + \rho} \tag{26}$$

where ρ donates a small positive constant.

However, using only the constant ρ cannot efficiently remove the chattering effect under various speed-regulation situations. Thus, ρ can be selected adaptively according to the speed tracking error [23]:

$$\rho = \rho_0 + \rho_1|E_k| \tag{27}$$

where ρ_0 and $\rho_1 > 0$ donate design coefficients.

Hence, the modified smooth function in equation (26) can be rewritten as:

$$\phi_k = \frac{S_k}{|S_k| + \rho_0 + \rho_1|E_k|} \tag{28}$$

For this kind of boundary layer technique, a tradeoff should be made between the tracking accuracy, robustness and chattering amplitude.

D. Stability Analysis

Substituting the final control law of equation (25) into equation (12), a simple calculation yields:

$$\begin{aligned} S_{k+1} &= MR_{k+1} - MAX_k - [MR_{k+1} - MAX_k - \\ &\quad MT\hat{d}_k + (G-M)E_k + \alpha TS_k + \beta T\operatorname{sgn}(S_k)] \\ &\quad -MTd_k + S_k + (G-M)E_k \\ &= S_k - [\alpha TS_k + \beta T\operatorname{sgn}(S_k) + p_k] \end{aligned} \tag{29}$$

with:

$$p_k = MT(d_k - \hat{d}_k) \tag{30}$$

It can be concluded from equations (22) and (23) that p_k is bounded with:

$$|p_k| \le M(\gamma_2 T^2 + \delta_2 \psi^{1/2} T) \tag{31}$$

Combined with the stability condition of the DSMC in [22], two cases for the stability analysis of the presented composite controller are discussed.

First, when $S_k \ge 0$, if the parameter satisfies the condition $\beta T > |p_k|$, it can be deduced from equation (29) that:

$$S_{k+1} = S_k - (\alpha TS_k + \beta T + p_k) < S_k \tag{32}$$

Otherwise, when $S_k < 0$, if the parameter satisfies the condition $\beta T > |p_k|$, it can be deduced from equation (29) that:

$$S_{k+1} = S_k - (\alpha TS_k - \beta T + p_k) > S_k \tag{33}$$

Therefore, combining the conclusions of equations (32) and (33), it can be summarized that:

$$|S_{k+1}| < |S_k| \tag{34}$$

with the sufficient condition:

$$\beta T > |p_k| \tag{35}$$

which means that under the constraint of equation (35), $|S_k|$ can decrease monotonously and the discrete sliding mode can be achieved within finite time steps. Thus, the stability of the presented composite controller can be assured.

An overall block diagram of the presented FTNDO-DISMC is depicted in Fig. 5, where the lumped disturbance

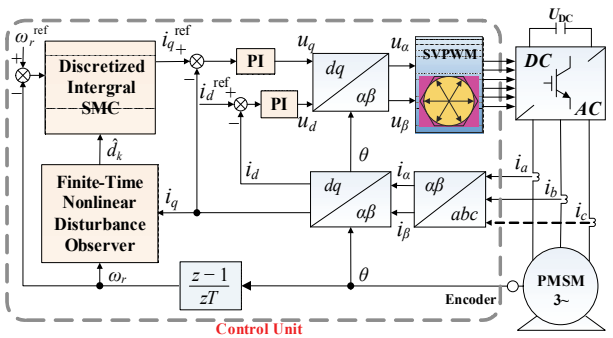

Fig. 5. Block diagram of the presented FTNDO-DISMC scheme.

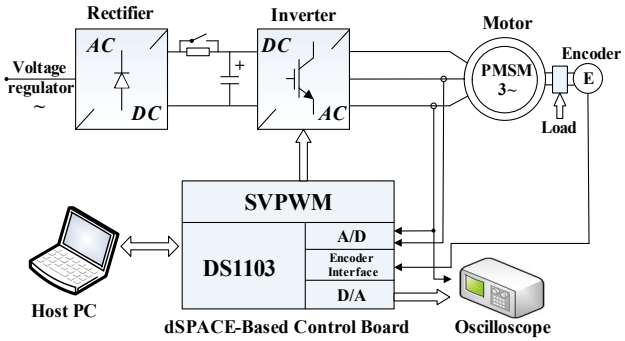

(a)

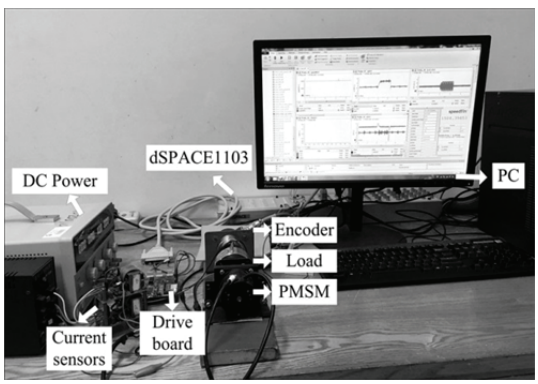

(b)

Fig. 6. Experimental setup: (a) Basic structure of the hardware system; (b) Photograph of the laboratory platform.

estimated by the FTNDO is taken as a feed forward link of the DISM controller for disturbance compensation. Moreover, according to equation (35), the switching gain is proportional to the estimation error, which is less than the actual disturbance in the conventional DSMC. Hence, to resist the same disturbance, the switching gain in the presented scheme is decreased, which indicates that the chattering and torque ripple of PMSMs can be reduced when compared with the conventional DSMC.

IV. Experimental Results

In this section, various experiments are investigated on a laboratory PMSM platform to verify the superiority of the presented FTNDO-DISMC scheme in terms of dynamic tracking responses and anti-disturbance capability.

A. Experimental Setup

The experimental setup for algorithm implementation is illustrated in Fig. 6, and the PMSM parameters are depicted in Table I. It can be observed that the laboratory platform consists of a PMSM and a control board. A 1024 P/R incremental encoder is installed for speed measurement. A biaxial hysteresis brake is used for the sudden injection and release of loads. Two Hall sensors are adopted for the measurement of the two phase currents.

The control algorithms are implemented on a DSP-based dSPACE DS1103 control board, with 16-bit ADC units and high-resolution incremental encoder interfaces. All of the experimental data are directly obtained from the ControlDesk software. The switching frequency of the PWM is set as 10 kHz and the sampling time is set as 0.1ms.

To ensure the safety of the system hardware, combined with the presented control scheme in Fig. 5, necessary current and voltage limitations that were presented in [2] are employed in this paper as below:

$$\begin{cases} i_d^{\text{ref}} = 0, \;\; i_q^{\text{ref}} \in [-I_m, \, I_m] \\ |\mathbf{u}| \le U_m \end{cases} \tag{36}$$

where i_d^{ref} and i_q^{ref} are d-q axes command currents. I_m is the rated amplitude of the phase current. **u** represents the command voltage vector composed of d-q axes voltages. U_m donates the maximum voltage limit depending on the DC bus voltage.

TABLE I
Parameters of a PMSM

Parameters	Values
DC bus voltage	48 V
Rated current	3 A
Rated speed	3000 rpm
Flux linkage	0.04 Wb
Rated power	125 W
Number of pole pairs	2
Stator line resistance	0.82 Ω
Stator line inductance	1.91 mH

Moreover, all of the parameters can be tuned online through the ControlDesk software. The parameter selection of the presented controller is given as follows. For the DISM controller, the parameter $M = 1$ can be chosen for the sake of simplicity, and the integral gain is $G > 0$. The reaching law parameter α should satisfy $0 < \alpha < 1/T$, and a larger α can increase the reaching rate. Increasing G or α can improve the dynamic responses. From equation (35), β should be selected as $\beta T > | p_k |$ to guarantee the robustness and stability of the controller. However, overlarge values of G, α and β can bring adverse control effects, such as chattering or overshoots. For the FTNDO, the parameters k_1 and k_2 can be easily tuned

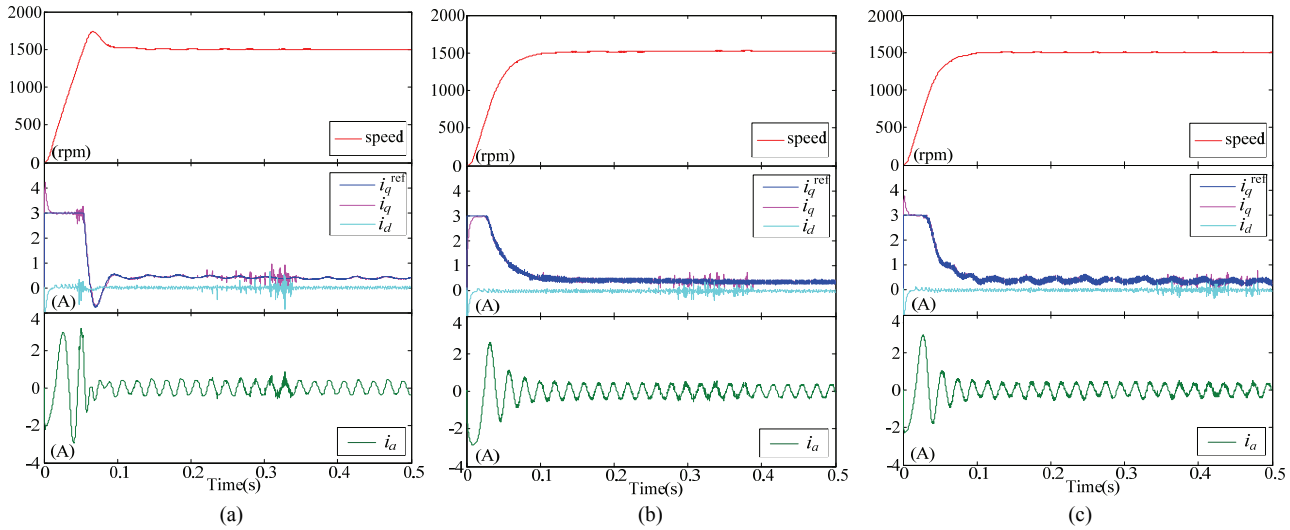

Fig. 7. Speed starting responses: (a) PI; (b) DISMC; (c) DISMC+FTNDO.

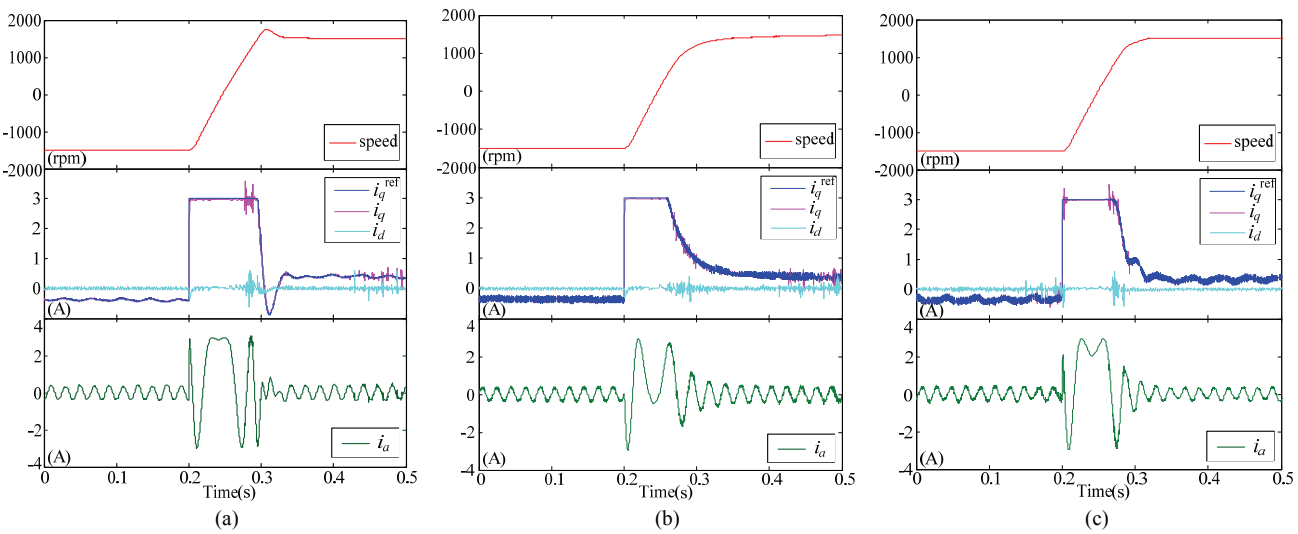

Fig. 8. Speed reversal responses: (a) PI; (b) DISMC; (c) DISMC+FTNDO.

since the behavior of the FTNDO is insensitive to them [13]. According to [20], easy choices for k_1 and k_2 are $k_1 = 1.5L^{0.5}$ and $k_2 = 1.1L$, where $L > 0$ is the only design parameter. This should also be adjusted according to the actual experimental results. Although a faster converging rate can be obtained by increasing L, the estimation error becomes more sensitive to the sampling time T_s and a tradeoff should be made between them. ρ_0 and ρ_1 can be selected as very small constants. The parameters of the presented controller are selected as $M = 1$, $G = 0.011$, $\alpha = 20$, $\beta = 25$, $k_1 = 2500$, $k_2 = 2\times10^6$, $\rho_0 = 0.5$ and $\rho_1 = 0.005$.

For comparison, the conventional discrete PI and DISMC controllers without the FTNDO are also employed. By using the Ziegler-Nichols method, the speed-loop PI parameters are tuned to the optimal values as $K_{pn} = 0.012$ and $K_{in} = 1.4$. The current-loop PI controllers are employed with parameters of $K_{pc} = 8$ and $K_{ic} = 2900$.

B. *Experimental Analysis*

First, experimental results of the speed starting responses using the PI, DISMC and DISMC+FTNDO are illustrated in Fig. 7, where the rotor speed, q-axis reference current i_q^{ref}, phase current i_a, and d-q axes feedback currents i_d and i_q are given. It can be seen that the speed starting responses using the DISMC and DISMC+FTNDO methods are similar, with shorter rising times and no explicit overshoots when compared with the PI control. It can also be seen that the presented controller has the best starting speed response.

Next, Fig. 8 shows the speed reversal responses from −1500 rpm to 1500 rpm. Similar conclusions can be drawn since the speed reversal performance using the presented control and the DISMC are better than that of the PI control.

Then, the anti-disturbance performance using the PI, DISMC and DISMC+FTNDO are compared in Fig. 9. The rated load is suddenly added at 1s and removed at 2s. It can

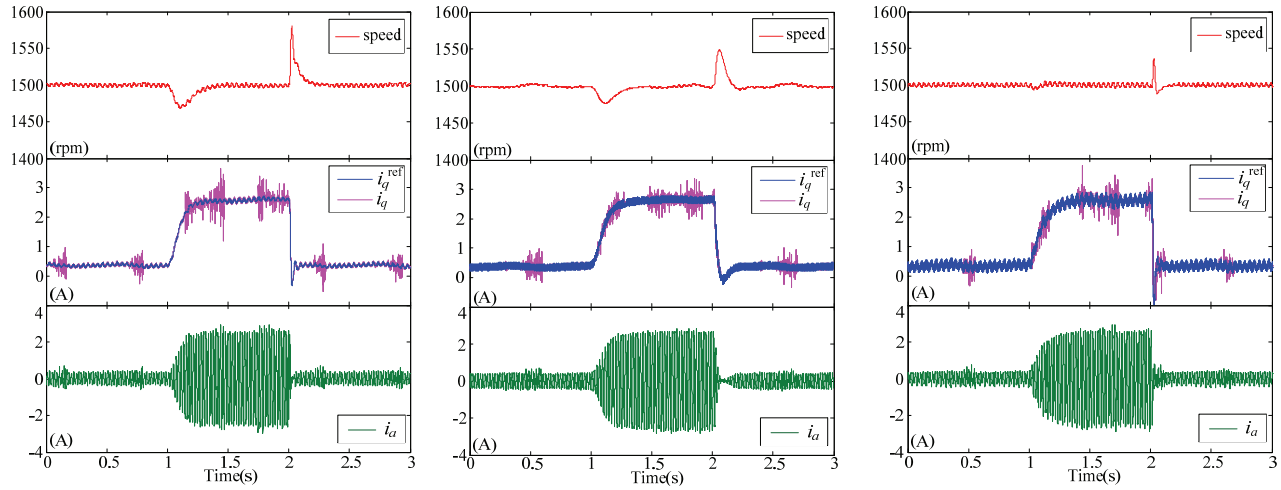

Fig. 9. Anti-disturbance capability when suddenly adding and removing the rated load: (a) PI; (b) DISMC; (c) DISMC+FTNDO.

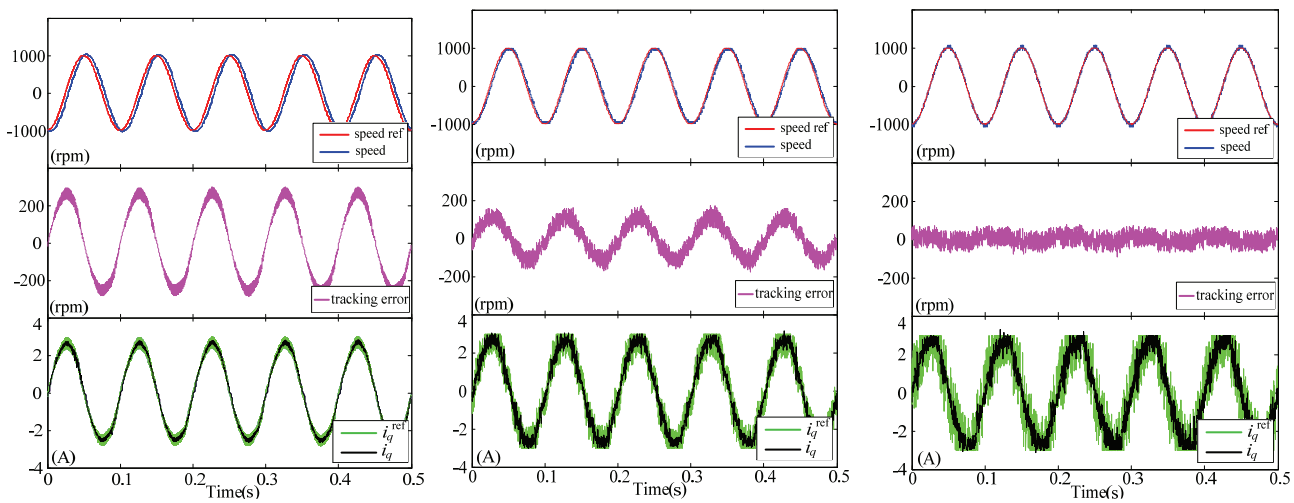

Fig. 10. 10 Hz sinusoidal speed tracking responses: (a) PI; (b) DISMC; (c) DISMC+FTNDO.

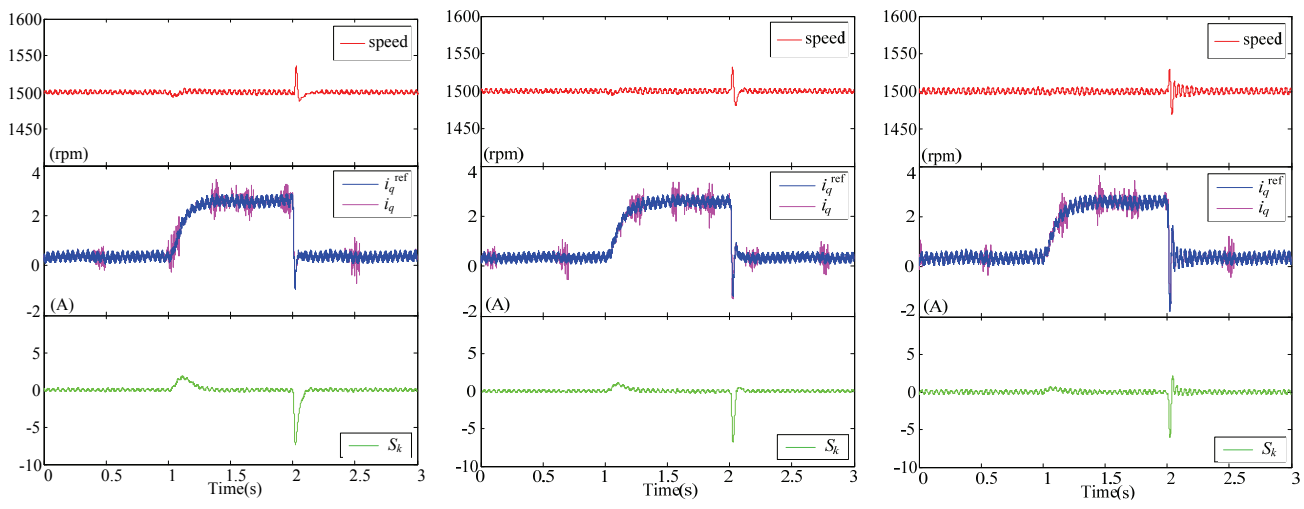

Fig. 11. Anti-disturbance capability of the presented controller with different values of α: (a) $\alpha = 20$; (b) $\alpha = 50$; (c) $\alpha = 100$.

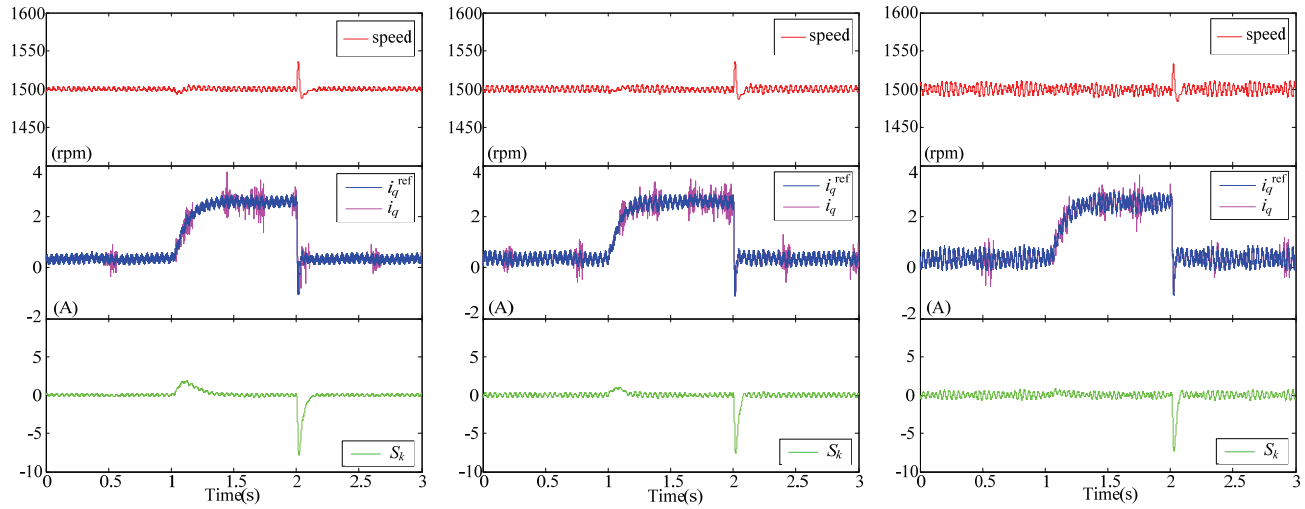

Fig. 12. Anti-disturbance capability of the presented controller with different values of β: (a) $\beta = 5$; (b) $\beta = 100$; (c) $\beta = 200$.

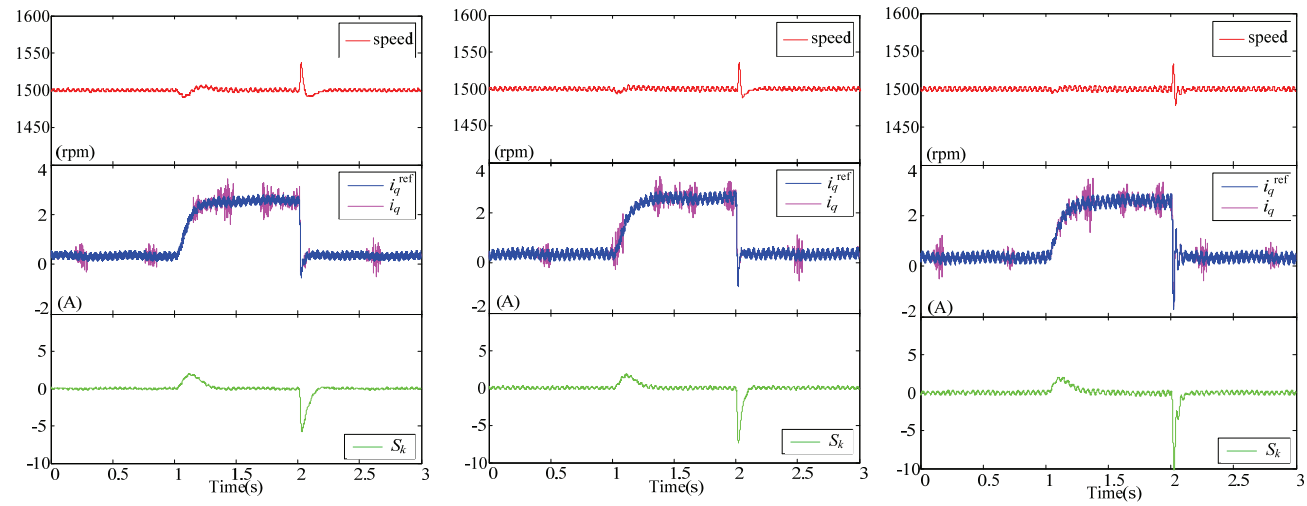

Fig. 13. Anti-disturbance capability of the presented controller with different values of G: (a) $G = 0.005$; (b) $G = 0.01$; (c) $G = 0.02$.

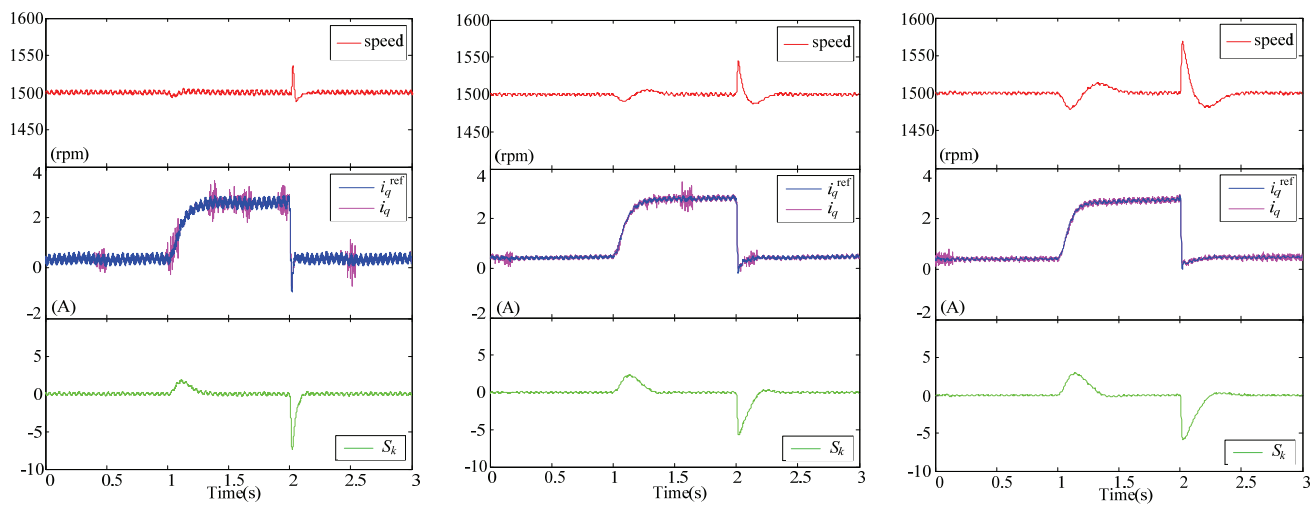

Fig. 14. Anti-disturbance capability of the presented controller with different values of T_s: (a) $T_s = 1\times10^{-4}$s; (b) $T_s = 5\times10^{-4}$s; (c) $T_s = 10^{-3}$s.

be seen that the maximum speed fluctuation with the presented controller is about 35 rpm, which is smaller than that using the PI and DISMC controllers at 50 rpm and 80 rpm, respectively. Moreover, after the occurrence of a disturbance, the speed recovery time with the DISMC+ FTNDO is the fastest. These results show that the speed robustness of the presented controller is the best among the three controllers.

To further verify the speed tracking performance of the presented controller, 10 Hz sinusoidal periodic speed tracking experiments are conducted and depicted in Fig. 10. It shows that the speed tracking error of the DISMC+FTNDO is the smallest at less than 100 rpm. In comparison, the speed tracking error of the DISMC and PI are about 200 rpm and 300 rpm, respectively. Hence, superior tracking responses can be obtained by using the presented controller.

Combined with the theoretical analysis, the anti-disturbance capability, chattering and adverse overshoots are highly dependent on the parameters α, β, G and the sampling time T_s. The control performance of the presented controller with different controller parameters are compared and shown in Figs. 11-13. In Fig. 11, different values of α are employed. Fig. 11 implies that increasing α can increase the approaching rate of the sliding surface S_k under load disturbances (faster responses). However, an overlarge α can induce larger adverse overshoots and chattering of the speed, i_q^{ref} and S_k. In Figs. 12 and 13, different values of β and G are employed. It can be seen that increasing β or G can improve the dynamic response and the disturbance rejection capability of the presented controller. However, an overlarge β or G can lead to a large chattering, and an overlarge G can bring about larger adverse overshoots of the speed and i_q^{ref}. Hence, to obtain the superior performance of the presented controller, a tradeoff should be made between the chattering amplitude and the robustness against disturbances.

Fig. 14 illustrates the anti-disturbance capability of the presented controller with different sampling times T_s under the condition that all of the parameters in the speed controller are kept constant. It can be seen that increasing T_s can decrease the convergence rate of S_k, i.e., it degrades the dynamic responses and robustness. However, the chattering significantly decreases with a larger T_s. In addition, by properly tuning the parameter G according to T_s, the presented controller can still obtain a superior control effect just like that with a small T_s.

The responses of the FTNDO and the convergence of the sliding surface S_k in the presented controller with rated load disturbances are shown in Fig. 15, which indicates that S_k can quickly reach the QSM after a disturbance occurs. Moreover, for the convenience of analysis, assuming that $B_f \approx 0$, the parameter perturbations are much smaller than the load variations and the acceleration is zero in equation (1) during the steady state. Then it can be deduced that the estimated

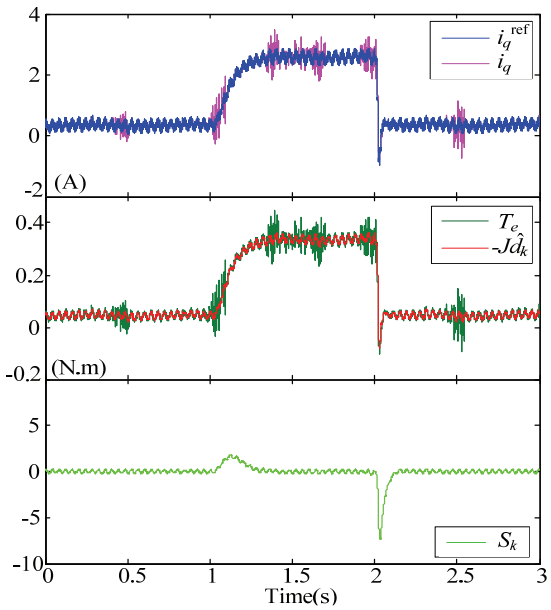

Fig. 15. Responses of the FTNDO and convergence of the sliding surface S_k in the DISMC with rated load disturbances.

disturbance is approximately equal to the electromagnetic torque T_e. Hence, by comparing T_e with the estimated load disturbance $-Jd(t)$ in equation (3), the observation performance of the FTNDO can roughly be determined. Fig. 15 shows that the FTNDO can accurately and quickly track actual disturbances in finite time steps.

V. Conclusions

This paper presented a FTNDO-DISM composite control scheme for PMSM drives. The main contributions of this work can be summarized as follows. (1) A reaching-law based DISM controller has been designed to enhance the dynamic responses and anti-disturbance capability of PMSM drives. By properly selecting the initial value of the discrete sliding function, the reaching process can be eliminated and the global robustness can be obtained. (2) A SMD-based discretized FTNDO has been presented to provide finite-time convergence estimation and compensation of the lumped disturbance. This can also alleviate the chattering without sacrificing robustness against parameter variations. (3) The FTNDO-DISM composite controller has been constructed and its stability has been analyzed theoretically. Experimental results have demonstrated the validity of the presented algorithm.

References

[1] X. Zhang, L. Sun, K. Zhao, and L. Sun, "Nonlinear speed control for PMSM system using sliding-mode control and disturbance compensation techniques," *IEEE Trans. Power Electron.*, Vol. 28, No. 3, pp. 1358-1365, Mar. 2013.

[2] M. Yang, X. Lang, J. Long, and D. Xu, "A flux immunity robust predictive current control with incremental model and extended state observer for PMSM drive," *IEEE Trans. Power Electron*., Vol. 32, No. 12, pp. 9267-9279, Dec. 2017.
[3] S. Li and Z. Liu, "Adaptive speed control for permanent-magnet synchronous motor system with variations of load inertia," *IEEE Trans. Ind. Electron*., Vol. 56, No. 8, pp. 3050-3059, Aug. 2009.
[4] J. W. Jung, V. Q. Leu, D. Q. Dong, H. H. Choi, and T. H. Kim, "Sliding mode control of SPMSM drivers-an online gain tuning approach with unknown system parameters," *J. Power Electron.*, Vol. 14, No. 5, pp. 980-988, Sep. 2014.
[5] X. Yu, B. Wang, and X. Li, "Computer-controlled variable structure systems: the state-of-the-art," *IEEE Trans. Ind. Electron.*, Vol. 8, No. 2, pp. 197-205, May 2012.
[6] J. Y. Humg, W. Gao, and J. C. Hung, "Variable structure control: a survey," *IEEE Trans. Ind. Electron*., Vol. 40, No. 1, pp. 2-22, Feb. 1993.
[7] M. L. Corradini, G. Ippoliti, S. Longhi, and G. Orlando, "A quasi-sliding mode approach for robust control and speed estimation of PM synchronous motors," *IEEE Trans. Ind. Electron.*, Vol. 59, No. 2, pp. 1096-1104, Feb. 2012.
[8] T. Bernardes, V. F. Montagner, H. A. Gründling, and H. Pinheiro, "Discrete-time sliding mode observer for sensorless vector control of permanent magnet synchronous machine," *IEEE Trans. Ind. Electron.*, Vol. 61, No. 4, pp. 1679-1691, Apr. 2014.
[9] K. Abidi, J. X. Xu, and Y. Xinghuo, "On the discrete-time integral sliding-mode control," *IEEE Trans. Autom. Contr.*, Vol. 52, No. 4, pp. 709-715, Apr. 2007.
[10] Z. Xi and T. Hesketh, "Discrete time integral sliding mode control for overhead crane with uncertainties," *IET Contr. Theory Appl.*, Vol. 4, No. 10, pp. 2071-2081, Oct. 2010.
[11] Q. Xu, "Adaptive discrete-time sliding mode impedance control of a piezoelectric microgripper," *IEEE Trans. Robot.*, Vol. 29, No. 3, pp. 663-673, Jun. 2013.
[12] H. Du, X. Yu, M. Z. Chen, and S. Li, "Chattering-free discrete-time sliding mode control," *Automatica*, Vol. 68, No. 6, pp. 87-91, Jun. 2016.
[13] A. Levant, "Higher-order sliding modes, differentiation and output-feedback control," *Int. J. Control*, Vol. 76, No. 9/10, pp. 924-941, Jan. 2003.
[14] A. Levant, "Sliding order and sliding accuracy in sliding mode control," *Int. J. Control*, Vol. 58, No. 6, pp. 1247-1263, Dec. 1993.
[15] L. Zhao, J. Huang, H. Liu, B. Li, and W. Kong, "Second-order sliding mode observer with online parameter identification for sensorless induction motor drives," *IEEE Trans. Ind. Electron.*, Vol. 61, No. 10, pp. 5280-5289, Oct. 2014.
[16] A. Levant, "Robust exact differentiation via sliding mode technique," *Automatica*, Vol. 34, No. 3, pp. 379-384, Mar. 1998.
[17] Y. B. Shtessel, I. A. Shkolnikov, and A. Levant, "Smooth second-order sliding modes: Missile guidance application," *Automatica*, Vol. 43, No. 8, pp. 1470-1476, Aug. 2007.
[18] W. H. Chen, J. Yang, L. Guo, and S. Li, "Disturbance-observer-based control and related methods-an overview," *IEEE Trans. Ind. Electron.*, Vol. 63, No. 2, pp. 1083-1095, Feb. 2016.
[19] Y. A. R. I. Mohamed, "Design and implementation of a robust current-control scheme for a PMSM vector drive with a simple adaptive disturbance observer," *IEEE Trans. Ind. Electron.*, Vol. 54, No. 4, pp. 1981-1988, Aug. 2007.
[20] J. Davila, L. Fridman, and A. Levant, "Second-order sliding-mode observer for mechanical systems," *IEEE Trans. Autom. Control*, Vol. 50, No. 11, pp. 1785-1789, Nov. 2005.
[21] R. P. Vieira, C. C. Gastaldini, R. Z. Azzolin, and H. A. Gründling, "Discrete-time sliding mode speed observer for sensorless control of induction motor drives," *IET Elect. Power Appl.*, Vol. 6, No. 9, pp. 681-688, Nov. 2012.
[22] S. Sarpturk, Y. Istefanopulos, and O. Kaynak, "On the stability of discrete-time sliding mode control systems," *IEEE Trans. Autom. Control*, Vol. 32, No. 10, pp. 930-932, Oct. 1987.
[23] T. L. Chern and Y. C. Wu, "Design of integral variable structure controller and application to electrohydraulic velocity servosystems," *IEE Proceedings D - Control Theory Appl.*, Vol. 138, No. 5, pp. 439-444, Sep. 1991.

Changming Zheng was born in China, in 1991. He received his B.S. degree in the College of Information and Control Engineering, China University of Petroleum (East China), Qingdao, China, in 2014, where he is presently working towards his Ph.D. degree. His current research interests include PMSM drives, renewable energy systems and nonlinear control applications.

Jiasheng Zhang was born in China, in 1957. He received his M.S. degree from Beihang University, Beijing, China; and his Ph.D. degree from Beijing Jiaotong University, Beijing, China. He is presently working as a Professor in the College of Information and Control Engineering, China University of Petroleum (East China), Qingdao, China. His current research interests include power electronics, AC motor drives, renewable distributed power sources and converters.